Quaternion Number Based Vanilla Recognition System

for Automating Polination

Ted Shaneyfelt, Sos Agaian, Mo Jamshidi
Electrical and Computer Engineering
The University of Texas at San Antonio
San Antonio, USA
ted.shaneyfelt@utsa.edu

Sevki Erdogan
Computer Science and Engineering
University of Hawaii at Hilo
Hilo, USA
serdogan@hawaii.edu

***Abstract*— Vanilla is the second most expensive spice worldwide. The high cost of vanilla has led to the problem of dangerous adulterated substitutes. Its high cost is attributed largely to the labor intensive hand pollination required where the melipona bee is not present. This article is the first known to present a machine vision system for the recognition of vanilla flowers and their stamen for pollination. We present a hypercomplex numbers based system. The present system is based on a rotational invariant basis more fitted to fast quaternion Fourier transform processing than Zernike Polynomial basis, and computer simulations. It could be used for other applications as well.**

***Keywords*— Agriculture, Machine vision, Farming, Image recognition, Signal processing, Robotics**

I. INTRODUCTION

Machine pollination has been successful with some other crops including tomatoes and dates. The methods differ significantly, as tomato plants only need to be vibrated to cause pollination [1]. Dates have different challenges, as they grow on larger palm trees. They are dusted either manually or robotically [2]. Vanilla orchid pollination is more complex. It requires a different technique altogether. The hand pollination of vanilla planifolia technique developed by Edmond Albius [3], [4] consists of locating and manipulating the area around the anther. The pollen must be carefully transferred along the column from the anther to contact the stigma [5]. Manual pollination is done using a small bamboo stick or toothpick. In nature, this is done by the melipona bee, which is found only in Mexico [6], making manual pollination necessary for vanilla to be cultivated throughout the rest of the world.

Hand pollination represents an estimated 40% of the cost of production the world's second most expensive spice [7], [8]. It has been said that pollination cannot be replicated by machine [9]. The high cost of manual labor has led to dangerous chemical imitations [10-12].

Recently quaternions have been used in the application of image processing [13-37]. Quaternions were first discovered by Hamilton in 1843 [38]. It is customary in quaternion color image processing to use the three dimensions of the composite color space. In 1988, Harris and Stevens presented a combined corner and edge detector [39], and the same year Noble presented a similar parameterless corner detector [40]. In 1998, Sochen used Beltrami color flow in a general framework for low level vision [41]. More recently, Jesús Angulo used the structure tensor of color quaternion image representations for invariant feature extraction [13].

This paper presents a hypercomplex numbers based system for color imaging with agricultural application in future robotic assisted pollination of vanilla planifolia. The system performs recognition of flowers and important features of their anatomy.

Section II provides background relating to hypercomplex numbers, Fourier basis functions, the quaternion Fourier Transform, and the Zernike polynomial as a function kernel. Section III presents the Special Quaternion Fourier kernel. Section IV proposes a vanilla planifolia image recognition system for robotic vision to be used in pollination. Section V is the conclusion.

II. BACKGROUND

This section presents mathematical background. Hypercomplex numbers, Fourier basis functions, the quaternion Fourier Transform, and the Zernike polynomial as a function kernel are all reviewed.

A. Hypercomplex Numbers

Hypercomplex numbers are extensions of the complex number system $c = x + yi$, $i^2 = -1$.

Quaternion numbers have the form

$$q = a + ri + gj + bk \tag{1}$$

Where i is unit red-ward displacement, j is unit green-ward displacement, and k is unit blue-ward displacement such that [38]

$$i^2 = j^2 = k^2 = ijk = -1 \tag{2}$$

The variables r, g, and b can be looked at as the corresponding amplitudes. The real value a is often assigned zero.

978-1-61284-471-8/11/$26.00 ©2011 IEEE

B. Quaternion Structure Tensor of an image

The eigenvalues of the structure tensor of an image are given by:

$$\frac{u_{xx}+u_{yy}\pm\sqrt{(u_{xx}-u_{yy})^2+(2u_{xy})^2}}{2} \quad (3)$$

Where *s,t* each indicate *x* or *y* so that u_{xx}, u_{xy}, u_{yy} are given by u_{st} in

$$u_{st} = \omega_\sigma * \left(\frac{\partial r}{\partial s}\frac{\partial r}{\partial t}\right) + \omega_\sigma * \left(\frac{\partial g}{\partial s}\frac{\partial g}{\partial t}\right) + \omega_\sigma * \left(\frac{\partial b}{\partial s}\frac{\partial b}{\partial t}\right) \quad (4)$$

$$\omega_\sigma = \left(2\pi\sigma^2 e^{j(x^2+y^2)}\right)^{-1} \quad (5)$$

Where the partial derivative of a color $f = r$ or $f = g$ or $f = b$ with respect to $s = x$ or $s = y$ is given by

$$\frac{\partial f}{\partial s} = \frac{\partial f}{\partial r}\frac{\partial r}{\partial s} + \frac{\partial f}{\partial g}\frac{\partial g}{\partial s} + \frac{\partial f}{\partial b}\frac{\partial b}{\partial s} \quad (6)$$

If we choose to use Angulo's saturation of [13] for a, we also have

$$\frac{\partial a}{\partial s} = \begin{cases} \frac{3}{2}\frac{\partial f_{max}}{\partial s} - \frac{\partial r}{\partial s} - \frac{\partial g}{\partial s} - \frac{\partial b}{\partial s}, & a \geq a_{med} \\ -\frac{3}{2}\frac{\partial f_{max}}{\partial s} + \frac{\partial r}{\partial s} + \frac{\partial g}{\partial s} + \frac{\partial b}{\partial s}, & a \leq a_{med} \end{cases} \quad (7)$$

C. Fourier basis functions

The classic 2D Fourier transform is defined as:

$$\hat{f}(u,v) = \sum_{x=0}^{M-1}\sum_{y=0}^{N-1} W_{uv}(x,y) f(x,y) \quad (7)$$

Where the Fourier transform kernel is defined as:

$$W_{mn}(x,y) = \frac{e^{-j2\pi\left(\frac{mx}{M}+\frac{ny}{N}\right)}}{\sqrt{MN}} \quad (9)$$

The Fourier Transform basis is illustrated in Figure 1 for further comparison.

There are several definitions of Quaternion Fourier Transform (QFT), including two-side, left-side, and right-side.

The Type 1 (two-side) QFT [42]:

$$\hat{f}_{(q1)}(u,v) \triangleq \frac{1}{MN}\sum_{x=0}^{M-1}\sum_{y=0}^{N-1} \frac{e^{-i2\pi\left(\frac{ux}{M}\right)}}{\sqrt{M}} f(x,y) \frac{e^{-j2\pi\left(\frac{vy}{N}\right)}}{\sqrt{N}} \quad (10)$$

Type 1 QFT uses a split basis:

$$W_{mn}(x,y) = \frac{e^{-i2\pi\left(\frac{mx}{M}\right)}}{\sqrt{M}}(\cdot)\frac{e^{-j2\pi\left(\frac{ny}{N}\right)}}{\sqrt{N}} \quad (11)$$

This basis is split into two sides as a result of the non-commutative property of quaternion multiplication.

The Type 2 (left-side) QFT:

$$\hat{f}_{(q2)}(u,v) \triangleq \frac{1}{MN}\sum_{x=0}^{M-1}\sum_{y=0}^{N-1} W_{uv}(x,y) f(x,y) \quad (12)$$

The Type 3 (right-side) QFT:

$$\hat{f}_{(q3)}(u,v) \triangleq \frac{1}{MN}\sum_{x=0}^{M-1}\sum_{y=0}^{N-1} f(x,y) W_{uv}(x,y) \quad (13)$$

Type 2 and 3 [43] (left and right-side) QFTs [44] use a simpler kernel defined simply by the substitution of the imaginary unit by a hypercomplex unit μ [43]:

$$W_{mn}(x,y) = \frac{e^{-\mu 2\pi\left(\frac{mx}{M}+\frac{ny}{N}\right)}}{\sqrt{MN}} \quad (14)$$

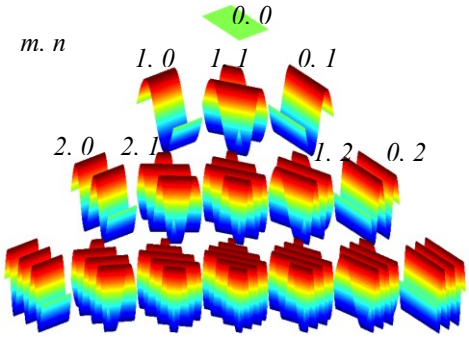

Figure 1. Fourier function (imaginary part)

D. Zernike Polynomials

The prime advantage often cited of the Zernike Polynomial is rotational invariance, though this invariance depends upon the predetermination of the axis of rotation and pre-scaling to a unit circle centered about that point. Zernike polynomials are given by the formula [45]:

$$R_{nm}(\rho) = \sum_{s=0}^{\frac{n-|m|}{2}} (-1)^s \frac{(n-s)!}{\left(\frac{n+m}{2}-s\right)!\left(\frac{n-m}{2}-s\right)!s!}\rho^{n-2s} \quad (15)$$

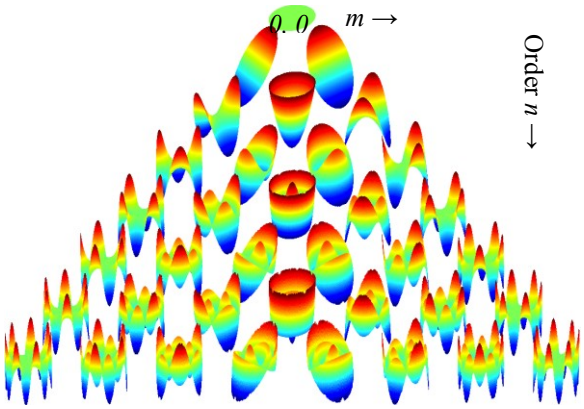

Figure 2. Zernike polynomials

In the radial basis of the Zernike Function in Figure 2 The rows represent increasing order n, and the columns m, with $m = 0$ in the center column. Properties of Zernike polynomials are listed in [46].

III. SPECIAL QFT KERNEL AND SOME PROPERTIES

This section introduces a special Quaternion Fourier Transform Kernel and some of its properties.

A. Proposed basis function

This system modifies QFT by using this special basis function for quaternions:

$$W_{mn}(\rho,\theta) = e^{-i2\pi\left(\frac{\rho}{M}\right)} + e^{-j\left(\frac{n\theta}{N}\right)} \quad (16)$$

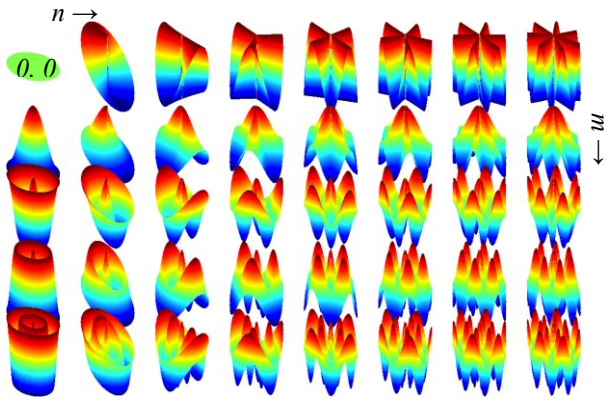

Figure 3. Proposed basis function

The special quaternion basis function illustrated in Figure 3 is comparable to other kernels.

1. Some Properties

Since the rotational orientation of orchid flowers vary somewhat as they grow, the rotational invariance property is important. A limit of the rotational invariance property is that it only holds around the pivot point of rotation. However, this is often overcome with extra processing by applying Zernike transforms around the neighborhood of each pixel in an image.

The basis function is composed of the sum of two sub-functions:

$$W_{mn}(\rho,\theta) = \mathrm{P}_{mn}(\rho) + \Theta_{mn}(\theta) \quad (17)$$

$$\mathrm{P}_{mn}(\rho) = e^{-i2\pi(\rho)};\ \Theta_{mn}(\theta) = e^{-j(n\theta)} \quad (18)$$

If the first term, $e^{-i2\pi(\rho)}$, affected only by the radius is rotationally invariant; and the second term, $e^{-j(n\theta)}$, affected only by the angle is also rotationally invariant, then their sum, $W_{mn}(\rho,\theta)$ must also be rotationally invariant.

Since the first term, $\mathrm{P}_{mn}(\rho) = e^{-i2\pi(\rho)}$ is a function only of radius, it follows that it must be rotationally invariant, as it contributes a circularly symmetric term to the sum.

Since the second term, $\Theta_{mn}(\theta) = e^{-j(n\theta)}$ is a periodic function, and an integral multiple of it is 2π, it is also circularly symmetric.

Since both terms are circular symmetric, their sum, $W_{mn}(\rho,\theta)$ is circularly symmetric, QED.

This can be seen also by inspecting the derivatives,

$$\frac{\partial}{\partial\theta}W_{mn}(\rho,\theta) = \frac{\partial}{\partial\theta}e^{-i2\pi(\rho)} + \frac{\partial}{\partial\theta}e^{-j(n\theta)} \quad (19)$$

$$\frac{\partial}{\partial\theta}W_{mn}(\rho,\theta) = \frac{\partial}{\partial\theta}e^{-jn\theta} = \frac{\mathrm{d}}{\mathrm{d}\theta}e^{-jn\theta} = -jne^{-jn\theta} \quad (20)$$

Fast computation of the transform is possible through the isomorphism of discrete Fourier transforms. Consider an $N \times N$ pixel image. Although the complexity of 2D Discrete Fourier Transform carried out directly on through matrix multiplication is $O(N^3)$, use of the Fast Fourier Transform reduces the complexity to $O(N^2 \lg N)$. This is fast compared to high order quaternion polynomial computation complexity.

Several "fast" algorithms [47] exist for order N quaternion moment calculation of an $N \times N$ pixel image. Gu's fast algorithm sacrifices accuracy due to round-off error in order to achieve $O(N^3)$ which is still worse than 2D FFT. More accurate "fast" algorithms exist at complexity $O(N^4)$ or higher.

IV. VANILLA RECOGNITION SYSTEM

This section presents a recognition system with application in vanilla recognition for machine pollination.

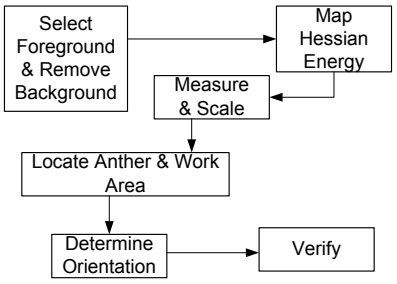

Figure 4. Recognition steps

This section describes a recognition system for the vanilla flower. The system provides the necessary coordinates relative to the camera of key features of the flower. The anther, which contains the pollen and must be manipulated, and work area within the labellum of the flower are identified and located by the system.

Recognition is performed in steps shown in Figure 4, according to key characteristics of the flower.

- *Select Foreground & Remove Background*: Size and color are used to select one flower to be further analyzed and to remove the background and other flowers. One flower is selected at a time to simplify the later steps of the problem. All other flowers
- *Map Hessian Energy*: The Hessian energy of the frills is used to locate the lip of the flower.
- *Measure & Scale*: Areas of high energy are used to determine the scale and location of the lip as a starting point for determining most relevant key points.
- *Locate Anther & Work Area*: Key points are selected that pinpoint the orientation of the lip and the work area. The work area is where a robotic manipulator can be maneuvered while pollinating.

- *Determine Orientation*: Orientation of the work area determined by key points in the work area and the relative position of the anther.
- *Verify*: A transform is used to verify characteristics of the image by different means provides confidence indicator for successful location.

These steps are illustrated in Figure 4 and described more in the following subsections.

The orchid flower is primarily yellow. The petals and sepals are all yellow, as are parts of the buds. Although some shades of yellow can be found in the flower that are distinct from the shades found in the buds, the distinction is not in itself a reliable indicator, as the flower itself is neither completely distinct colors, nor are the characteristic colors much different from those of the buds. For recognition purposes, an individual flower must be separable from buds and other flowers which may be in view. It is common for bud to be in the vicinity of a flower, as shown in Figure 5.

Figure 5. Vanilla flower and buds, courtesy Jim Reddekopp and HVC

Histogram techniques are used to determine areas which are characteristic of the flower, categorized as typifying foreground, vs. typical background colors by training on a set of images with regions designated as target background regions. The histogram is smoothed using a Gaussian spread function. This is done to compensate for quantization noise or introduced by the camera and encoding of the image. Furthermore, the weighted background histogram is subtracted from the foreground histogram. After training complete and histograms are prepared, live recognition is performed using the histograms of foreground and background images.

A copy of the image to be recognized is first morphologically opened and closed. This reduces the noise of small areas of similar colors appearing in nearby buds and stems, which might otherwise deform the selection shape of the flower to be recognized, and add energy noise to the subject being selected.

The modified image is then scanned linearly for a long consecutive run of qualifying pixels. A pixel is qualifying if its color is not normally found in the background regions, i.e. the background histogram count is below a threshold near zero. Considerable overlap occurs between natural foreground and background regions, but there are also areas characteristic of each region. Additional pixels are qualifying if they sometimes occur in the foreground. A run is ended when a pixel that never occurred in the flower's color-space in the training data is encountered. The location of the maximum run-length and location are used to select a flower. The result of this process is a point within one of the larger and likely nearby fully blooming flowers in the image.

After this process, the modified image is filled around the point of the high intensity pixel. This works because the flower is higher intensity than any other large portions of the plant. Furthermore, since only one vanilla flower blooms on a given day on any raceme, the flowers do not tend to group in bunches, making this algorithm well suited for vanilla orchids in particular. The resulting area identifies the orchid flower's boundaries with smooth contours.

Once the boundaries are determined, everything else is removed from the image. Thus background noise removal is complete, and an image of a selected foreground flower remains in isolation, as shown in Figure 6.

Figure 6. Backgrond removal

The area to be manipulated in vanilla pollination is entirely surrounded by the characteristic lip of the flower, which is formed by a single unique petal. An important characteristic of the vanilla is the high frequency waves or frills around the edge of the lip petal. The yellow on the lip also may be a deeper more saturated yellow than the rest of the flower or any of the buds. The lip flattens out in appearance at the bottom to form a landing pad below the column, where a work area normally used by a melapona bee in the process of pollination could be used by a robotic manipulator as a work area.

In this paper, we follow the technique of [13]. The structure tensor of color quaternion image representation technique has proved successful in invariant feature extraction. It is relied upon heavily in this process as it provides good results for several steps in vanilla recognition.

The high energy concentration around the lip petal is used to locate it. The focus is next turned toward the shape and orientation of the lip by examining the area near the center of

energy. That center of energy is found by taking the maximum of the resulting energy of the image smoothed with a Gaussian spread function. The energy of the image in Figure 6 is shown in Figure 7, with the center marked surrounding the radius set according to a threshold on the smoothed energy function.

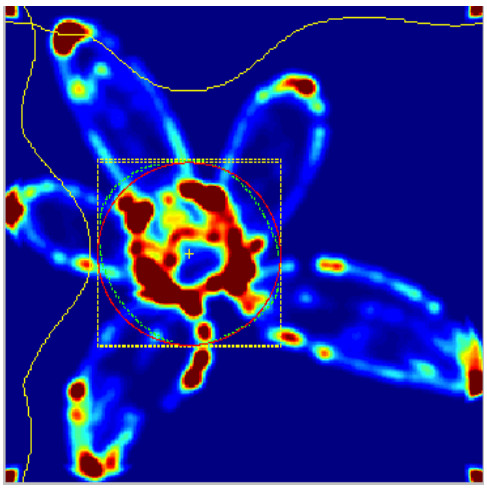

Figure 7. Energy

The anther appears much less saturated and lighter in color than the surrounding area. It is centered above the work area when the flower is oriented with the landing pad horizontally at the bottom of the frame of reference. This object must be locatable in order to manipulate it.

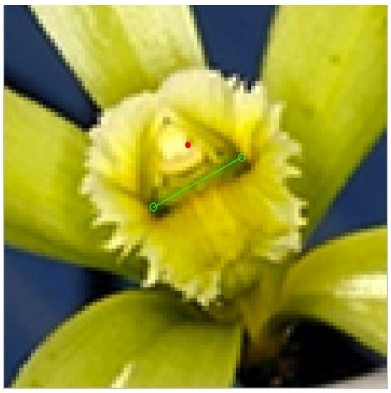

Figure 8. Key points selected: Work area (indicated by a green line) and pollination target (indicated by a red dot).

Having used the energy to locate the lip petal, our attention is turned toward its orientation. For this, we make use of key points within the lip. Key point selection is performed using the energy according to [13]. Corners are characterized by the values of eigenvalues of the tensor matrix being nearly equal to one another. Nearby values to the left and right are chosen which often correspond to the shadows at the left and right ends of the work area. The results will be further cross-checked later. At this point, they are measured, and their center-point is determined to be the revised center of the image. The nearby point above the center-point, considering the orientation given by the left and right shadow vertices is a candidate for the anther cap. The resulting points for the same image are presented in Figure 8.

The key points shown indicate the work area with a solid line, and the target point of the anther cap indicated with the dot. These are the desired points to recognize for pollination purposes. It remains to verify that these points are correct.

Orientation uses a method inspired by Zernike moments. Zernike moments form a basis on the unit circle.

$$\rho = \sqrt{x^2 + y^2} < 1, \quad \theta = \tan^{-1}\frac{y}{x} \tag{21}$$

$$V_{nm}^{\circ}(\rho, \theta) = R_{nm}(\rho)e^{jm\theta} \tag{22}$$

Or in Cartesian form:

$$V_{nm}^{\times}(x, y) = V_{nm}^{\circ}\left(\sqrt{x^2 + y^2}, \tan^{-1}\frac{y}{x}\right) \tag{23}$$

However, since the points selected, are not helpful for our purposes, we either modify the method or use it differently than in the classical application. Rotational invariant properties of Zernike polynomial are desirable since the flowers often grow rotated up to 30 degrees. Rotated images have the same coefficients except for a phase difference. This feature could be used to both identify a rotated image and determine its rotational orientation. It would seem that quaternion color representation may be useful if it could be applied along with Zernike polynomials, or if a similar representation could be found in which the concepts could be combined.

However, this basis does not feature the rotational invariance of the Zernike polynomial basis. To extend the Zernike or a similar transform with rotational invariance, a kernel function with sinusoidal variation in two parameters is sought.

This basis function is used to independently verify the results of the previous step. When using the special basis is used, cross correlation identifies the phase. Phase determines the rotational orientation. This orientation is compared to the rotation result of the measurement step. If the results are nearly equal and the correlation is high, the image is likely identified correctly.

A method has been presented for identifying the key points necessary for navigating a robot manipulator to the desired location for pollination of vanilla planifolia. The method was used with images rotated at orientations ranging from -45 to 45 degrees. The images are reliably successfully identified between -30 degrees and 30 degrees, and unreliably up to -45 to 45 degrees, with error being reliably detected in the verification step. Future research required to make long term goals of commercialization, and revolutionizing of the vanilla industry possible.

V. Conclusion

High cost of labor intensive pollination has led to inferior synthetic substitutes entering the market. This paper presents an alternative to the costly hand pollination. A system has been presented for machine recognition of the flower to facilitate future robotic pollination. Simulation results suggest that flower recognition can be performed, enabling machine assisted pollination to be developed.

ACKNOWLEDGMENT

To Jim Reddekopp and the Hawaiian Vanilla company for their inspiration, provision of images, to Jesús Angulo for his inspiration and assistance with hypercomplex energy analysis; to Luca Costantini for his assistance with Zernike analusis be grateful thanks. Their contribution has been indispensable in this research.

REFERENCES

[1] G. Hochmuth, "Production of Greenhouse Tomatoes - Florida Greenhouse Vegetable Production Handbook, Vol 3," Horticultural Sciences Department, Florida Cooperative Extension Service, Institute of Food and Agricultural Sciences, University of Florida, 2001.

[2] A. Shapiro et al., "Draft: A Robotic Protoype for Spraying and Pollinating Date Palm Trees," in *Proceedings of the 9th Biennial ASME Conference on Engineering Systems Design and Analysis*, 2008.

[3] J. G. Fouché and L. Jouve, "Vanilla planifolia: history, botany and culture in Reunion island," *Agronomie*, vol. 19, no. 8, pp. 689-703, 1999.

[4] T. Ecott, *Vanilla: Travels in Search of the Ice Cream Orchid*. New York: Grove Press, 2004.

[5] T. D. Whippie, "Vanilla planifolia - An Adventure in Pollination," *The McAllen International Orchid Society Journal*, vol. 10, no. 5, pp. 2-6, May. 2009.

[6] M. Evans, "Vanilla Odyssey," *Gastronomica*, vol. 6, no. 2, pp. 91-93, 01-Apr-2006.

[7] H. Panda, "Vanilla - World's second-most expensive spice," in *Aromatic Plants Cultivation, Processing And Uses*, New Delhi: Asia Pacific Business Press, Inc., 2005, pp. 61-71.

[8] C. Westerkamp and G. Gottsberger, "The costly crop pollination crisis," *Pollination bees: the conservation link between agriculture and nature. Brasília, Ministry of Environment, Secretariat for Biodiversity and Forests*, pp. 51–56, 2002.

[9] "Hawaiian Vanilla Company." [Online]. Available: http://www.hawaiianvanilla.com/hvc_media.asp. [Accessed: 20-Mar-2010].

[10] J. D. Bythrow, "Vanilla as a Medicinal Plant," in *Seminars in Integrative Medicine*, vol. 3, pp. 129–131, 2005.

[11] R. J. Marles, C. É. Compadre, and N. R. Farnsworth, "Coumarin in vanilla extracts: its detection and significance," *Economic Botany*, vol. 41, no. 1, pp. 41–47, 1987.

[12] L. S. de Jager, G. A. Perfetti, and G. W. Diachenko, "Determination of coumarin, vanillin, and ethyl vanillin in vanilla extract products: liquid chromatography mass spectrometry method development and validation studies," *Journal of Chromatography A*, vol. 1145, no. 1, pp. 83–88, 2007.

[13] J. Angulo, "Structure Tensor of Colour Quaternion Image Representations for Invariant Feature Extraction," in *Computational Color Imaging*, p. 100, 2009.

[14] J. Wang and L. Liu, "Specific color-pair edge detection using quaternion convolution," in *Image and Signal Processing (CISP), 2010 3rd International Congress on*, vol. 3, pp. 1138–1141, 2010.

[15] B. Chen, H. Shu, H. Zhang, G. Chen, and L. Luo, "Color Image Analysis by Quaternion Zernike Moments," in *2010 20th International Conference on Pattern Recognition*, pp. 625-628, 2010.

[16] C. Xie and B. V. Kumar, "Quaternion Correlation Filters for Color Face Recognition," p. 9, 2005.

[17] L. Shi and B. Funt, "Quaternion color texture segmentation," *Computer Vision and Image Understanding*, vol. 107, no. 1, pp. 88-96, Jul. 2006.

[18] S. J. Sangwine, "Colour Image Edge Detector Based on Quaternion Convolution," *Electronics Letters*, vol. 34, no. 10, pp. 969-971, May. 1998.

[19] S. C. Pei and C. M. Cheng, "Color image processing by using binary quaternion-moment-preserving thresholding technique," *IEEE Transactions on Image Processing*, vol. 8, no. 5, pp. 614–628, 1999.

[20] T. A. Ell and S. J. Sangwine, "Hypercomplex Fourier Transforms of Color Images," *IEEE Transactions on Image Processing*, vol. 16, no. 1, pp. 22-35, 2007.

[21] C. Cheng and S. Pei, "Sub-Pixel Color Edge Detection by Using Binary ` Quaternion-Moment-Preserving Thresholding Technique," *IEEE*, 1998.

[22] D. Assefa, L. Mansinha, K. F. Tiampo, H. Rasmussen, and K. Abdella, "Local quaternion Fourier transform and color image texture analysis," *Signal Processing*, 2009.

[23] L. Shi and B. Funt, "Quaternion color texture segmentation," p. 9, 2007.

[24] S. C. Pei and C. M. Cheng, "A novel block truncation coding of color images using a quaternion-moment-preserving principle," *IEEE Transactions on Communications*, vol. 45, no. 5, pp. 583–595, 1997.

[25] S. C. Pei, J. H. Chang, and J. J. Ding, "Quaternion matrix singular value decomposition and its applications for color image processing," in *IEEE Internat. Conf. on Image Processing (ICIP)*, pp. 805–808, 2003.

[26] J. Chang, S. Pei, and J. Ding, "2D Quaternion Fourier Spectral Analysis and its Applications," presented at the 2004 IEEE International Symposium on Circuits and Systems, Piscataway N.J., pp. 241-244, 2004.

[27] S. J. Sangwine and T. A. Ell, "Hypercomplex Fourier Transforms of Color Images," *IEEE*, 2001.

[28] S. DelMarco, "Multiple Template-Based Image Matching Using Alpha-Rooted Quaternion Phase Correlation," 2010.

[29] E. Bayro-Corrochano, N. Trujillo, and M. Naranjo, "Quaternion Fourier Descriptors for the Preprocessing and Recognition of Spoken Words Using Images of Spatiotemporal Representations," *Journal of Mathematical Imaging and Vision*, vol. 28, no. 2, pp. 179-190, 2007.

[30] S. DelMarco, "Multiple template-based image matching using alpha-rooted quaternion phase correlation," presented at the Mobile Multimedia/Image Processing, Security, and Applications 2010, Orlando, Florida, USA, pp. 77080F-77080F-11, 2010.

[31] Y. Lei, C. chen, and F. Lang, "Quaternion singular Value Decomposition Approach to Color Image De-noising," in *Proceedings of the International Joint Conference on Neural Networks*, 2008.

[32] W. Feng, B. Hu, and C. Yang, "A Subpixel Color Image Registration Algorithm Using Quaternion Phase-only Correlation," 2008.

[33] W. Feng, B. Hu, and C. Yang, "A Quaternion Phase-Only Correlation Algorithm for Color Images," in *Proceedings - International Conference on Image Processing, ICIP*, pp. 461-464, 2008.

[34] \. N. Subakan and B. C. Vemuri, "Color Image Segmentation in a Quaternion Framework," in *Proceedings of the 7th International Conference on Energy Minimization Methods in Computer Vision and Pattern Recognition*, p. 414, 2009.

[35] L. Shi and B. Funt, "Quaternion Colour Texture," presented at the Tenth Congress of the International Colour Association AIC Colour, Granada, Spain, 2005.

[36] C. Yang, J. Zhang, X. Xu, H. Chang, and G. He, "Quaternion phase-correlation-based clutter metric for color images," p. 7, 2007.

[37] W. Feng, B. Hu, and C. Yang, "A quaternion phase-only correlation algorithm for color images," in *15th IEEE International Conference on Image Processing, 2008. ICIP 2008*, pp. 461–464, 2008.

[38] W. R. Hamilton, "$i^2 = j^2 = k^2 = ijk = -1$," in *carved in stone*, 1843.

[39] C. Harris and M. Stephens, "A Combined Corner and Edge Detector," in *Proceedings of the 4th Alvey Vision Conference*, pp. 147-151, 1988.

[40] J. A. Noble, "Finding corners," *Image and Vision Computing*, vol. 6, no. 2, pp. 121-128, May. 1988.

[41] N. Sochen, R. Kimmel, and R. Malladi, "A general framework for low level vision," *IEEE Transactions on Image Processing*, vol. 7, no. 3, pp. 310-318, 1998.

[42] M. Felsberg and G. Sommer, "Optimized fast algorithms for the quaternionic Fourier transform," *Lecture notes in computer science*, pp. 209–216, 1999.

[43] S. C. Pei, J. J. Ding, and J. H. Chang, "Efficient implementation of quaternion Fourier transform, convolution, and correlation by 2-D complex FFT," *IEEE Transactions on Signal Processing*, vol. 49, no. 11, pp. 2783–2797, 2001.

[44] T. A. Ell and S. J. Sangwine, "Decomposition of 2D hypercomplex Fourier transforms into pairs of complex Fourier transforms," in *Proc. EUSIPCO*, pp. 151–154, 2000.

[45] P. Fricker, "Analyzing LASIK Optical Data Using Zernike Functions," *MATLAB Digest*, pp. 1-6, Jan-2008.

[46] Y. Bin and P. Jia-Xiong, "Invariance analysis of improved Zernike moments," *Journal of Optics A: Pure and Applied Optics*, vol. 4, pp. 606–614, 2002.

[47] G. Amayeh, A. Erol, G. Bebis, and M. Nicolescu, "Accurate and efficient computation of high order zernike moments," *Advances in Visual Computing*, pp. 462–469, 2005.